

Development and Performance Study of Polypropylene/Polyester Bicomponent Melt-Blowns for Filtration

Ya Liu,¹ Bowen Cheng,² Na Wang,¹ Weimin Kang,¹ Weili Zhang,³ Keqi Xing,³ Wenjuan Yang³

¹School of Textiles, Tianjin Polytechnic University, Tianjin 300160, People's Republic of China

²School of Materials Science and Engineering, Tianjin Polytechnic University, Tianjin 300160, People's Republic of China

³Taida Clean Material Company, Limited, of Tianjin, Tianjin 300400, People's Republic of China

Received 24 August 2010; accepted 4 May 2011

DOI 10.1002/app.34861

Published online 4 October 2011 in Wiley Online Library (wileyonlinelibrary.com).

ABSTRACT: In this study, a new type of polypropylene (PP)/polyester (PET) bicomponent melt-blown (bi-MB) for filtration was developed through the melt-blowing process with raw materials of melt-blown (MB)-grade PP and PET chips. The structure, porosity, and filtration performance of the bi-MBs were tested through relevant instruments. The results show that the average fiber diameter in the bi-MBs was 2–3.5 μm , the average pore size was 12.3–15.6

μm , and the porosity was 90–94%. The results also show that the filtration efficiency of the bi-MBs was much higher than that of monocomponent PP MBs. It reached the highest value of 97.34% when the PP/PET ratio was 50/50 and could be used as high-performance filter media. © 2011 Wiley Periodicals, Inc. *J Appl Polym Sci* 124: 296–301, 2012

Key words: fibers; polyesters; poly(propylene) (PP)

INTRODUCTION

The term *bicomponent* usually refers to fibers that are formed by two polymers extruded separately from at least two extruders but spun together through the orifices. The configuration of such a bicomponent fiber may be a sheath/core arrangement, wherein one polymer is surrounded by another, or a side-by-side or other sectional configuration.¹

Bicomponent melt-blown (bi-MB) technology was developed in the 1980s, and it made rapid progress in this recent decade.² It was mainly developed in America, Japan, and Germany. Companies such as Reifenhauer, Kasen, Chisso, Hills, and Nordson have made outstanding contributions to bi-MB technology, and nowadays, they are the main companies that provide new bi-MB technology and product lines.^{3–6}

Since 2002, Zhang and coworkers^{7–10} have studied bi-MBs in the laboratory. They have focused on the splitting process for the bicomponent fibers. All of these studies have been done in the laboratory stage and with no progress on commercial production.

There has been no other report on bi-MBs after that. With MB-grade polypropylene (PP) and polyester (PET) resin chips, a new type of PP/PET bi-MB for filtration was developed through a product line in Taida Clean Material Co., Ltd., of Tianjin, China.

In this study, the performances of the new type PP/PET bi-MBs were examined; we studied the pore size, porosity, air permeability, filtration efficiency, and so on. The results show the advantages of the PP/PET bi-MBs compared to monocomponent (mono) PP MBs and that they could be used as high-performance filter media.

PROCESS OF PP/PET bi-MBs

Raw material

MB-grade PP was produced by Longkou Daoen Engineering Plastic Co., Ltd. (Shandong, China). The melt flow index was 1000 g/10 min.

MB-grade PET was produced by Eastman Co. (Kingsport, Tennessee, the United States). The melt temperature was 257°C, and the apparent viscosity was 30 Pa·s at 310°C.

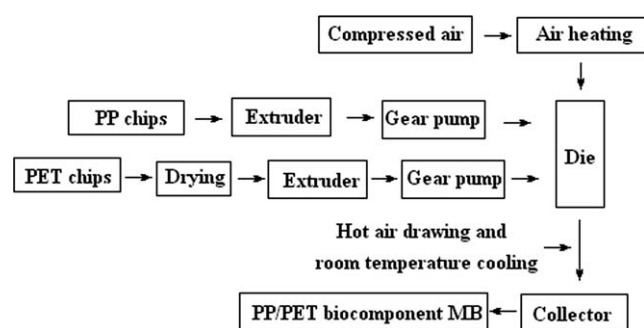
Product line and flow chart

The bi-MBs were produced through the bi-MB line made by Nordson Co. (Amherst, Ohio, the United States) in Taida Clean Material Co. (Tianjin, China). The following flow chart shows the synthesis process:

Correspondence to: Y. Liu (liuya8353@163.com).

Contract grant sponsor: Tianjin Municipal Science and Technology Commission; contract grant number: 07ZCKFGX03100.

Contract grant sponsor: National 863 Projects; contract grant number: 2007AA03Z359.



The theory of the bi-MB process was just like that of the mono PP MBs. The schematic of the side-by-side bi-MB lines is shown in Figure 1.

At the fixed parameters shown in Table I, the PP/PET side-by-side bi-MBs with ratios of 30/70, 50/50, and 70/30 of PP to PET were successfully produced through control of the rotary speed of metering pumps from 25 to 35 rpm. The basic weight was 35 g/m².

PERFORMANCE TEST

The morpha structure, fiber diameter, and distribution, average pore diameter, and mechanical and filtration performances of the PP/PET bi-MBs were tested according to relative methods.

Test of the morpha structure and average fiber diameter

A KYKY-2800 scanning electron microscope (Scientific Apparatus Co., Chinese Academy of Sciences, Beijing, China) was used to observe the structures of the bi-MBs, and ipwin32 software was used to measure the fiber diameter in the bi-MBs.

Test of the mean pore diameter and calculation of porosity

A pore size meter (PSM 165) (Topas GmbH, Dresden, Germany) was used to test the mean pore size in the bi-MBs. The measurement principle of the PSM 165 was capillary flow analysis. The mean pore diameter was the diameter according to the bubble-point pressure when half of the pores in the filter media were opened.

The porosity of the bi-MBs was calculated with eq. (1):¹¹

$$n = \left(1 - \frac{m}{\rho\delta}\right) \times 100\% \quad (1)$$

where n is the porosity (%), m is the mass per square meter (g/m²), ρ is the density of raw material (g/cm³), and δ is the thickness of MB (m). For the bi-MBs, ρ was calculated with eq. (2):

$$\rho = \rho_1 s_1 + \rho_2 s_2 \quad (2)$$

where ρ_1 is the density of PP ($\rho_1 = 0.91$ g/cm³), s_1 is the percentage of PP, ρ_2 is the density of PET ($\rho_2 = 1.38$ g/cm³), and s_2 is the percentage of PET.

Test of the mechanical performance

A YG065 electronic fabric strength machine (Electronic Apparatus Co., Laizhou, China) was used to test the mechanical performances of the bi-MBs.

Test of the filtration performance and air permeability

A CLJ-0.3A laser particle arithmometer (Clean Technology Research Institute, Suzhou, China) was used to test the filtration efficiencies and pressures of the bi-MBs. A number of the particles of every grade flowing through the testing machine could be read (t). After we put the sample in the testing machine, another measurement of the number of particles of every grade flowing through the testing machine could be read (t_1). The filtration efficiency (FE) was calculated with eq. (3):

$$FE = \frac{t - t_1}{t} \times 100\% \quad (3)$$

Also, the filtration resistance could be read through the testing machine.

A YG461 air permeability apparatus (Textile Apparatus Co. Ningbo, China) was used to test the air permeability of the bi-MBs.

RESULTS AND DISCUSSION

Structure

Figure 2 shows the scanning electron microscopy (SEM) images of different ratio PP/PET bi-MBs.

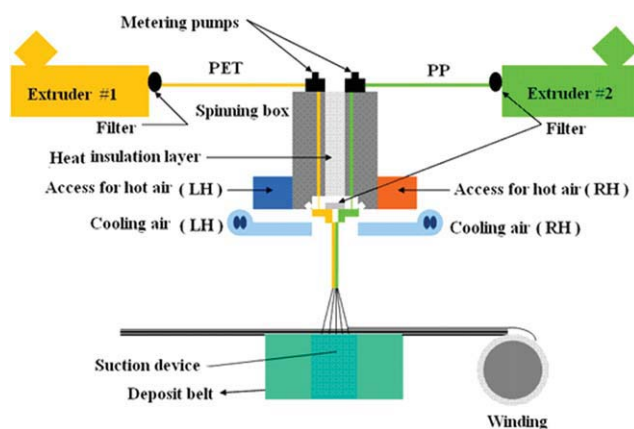


Figure 1 Schematic of the side-by-side bi-MB lines: (a) PP/PET 30/70, (b) PP/PET 50/50, (c) PP/PET 70/30, and (d) PP/PET 100/0. LH = left hand; RH = right hand. [Color figure can be viewed in the online issue, which is available at wileyonlinelibrary.com.]

TABLE I
Main Parameters of the MB Process

	Spinning temperature (°C)	Hot-air temperature (°C)	Die-to-collector distance (cm)	Belt speed (m/min)
PET	310	315	25	12
PP	290			

From Figure 2(a–c), we could see that each fiber in the bi-MBs was composed of two components, PP and PET. They formed a three-dimensional netted structure. Also, the fiber diameter in the bi-MBs was finer than that in the pure PP MBs. During the process of fiber formation, the PP and PET melts had different thermal performances. They showed different shrinkage properties during the cooling stage, so the two components in the bicomponent fiber split into finer fibers and formed the crimp fibers. However, without the outside force, the fibers could not be separated entirely. The performance of bi-MB fibers enabled the higher fluffy, softer, and antipene-

trative performance of the bi-MBs. Meanwhile, the bigger specific surface area of the fiber was formed.

Average fiber diameter

Ipwin32 software was used to measure the fiber diameter in the bi-MBs SEM images. The average diameters were calculated according to 50 measurements, and the distribution of the fiber diameter is shown in Figure 3.

It can be seen from Figure 3 that the average fiber diameter of the pure PP MBs was 4.6 μm , and it decreased to 2–3.5 μm in the PP/PET bi-MBs. Among these bi-MBs, the fiber diameter reached the lowest value of 2.34 μm at the ratio of 50/50 PP/PET. When there was only PP in the fiber, it could not be split at all, so the fiber diameter was thicker. When there were two components, PP and PET, in one fiber, some of the fibers split during the fiber-drawing stage, and the fiber diameter turned finer. However, when there was 70% PP or PET, most of the fiber diameter was thicker than those with 50%

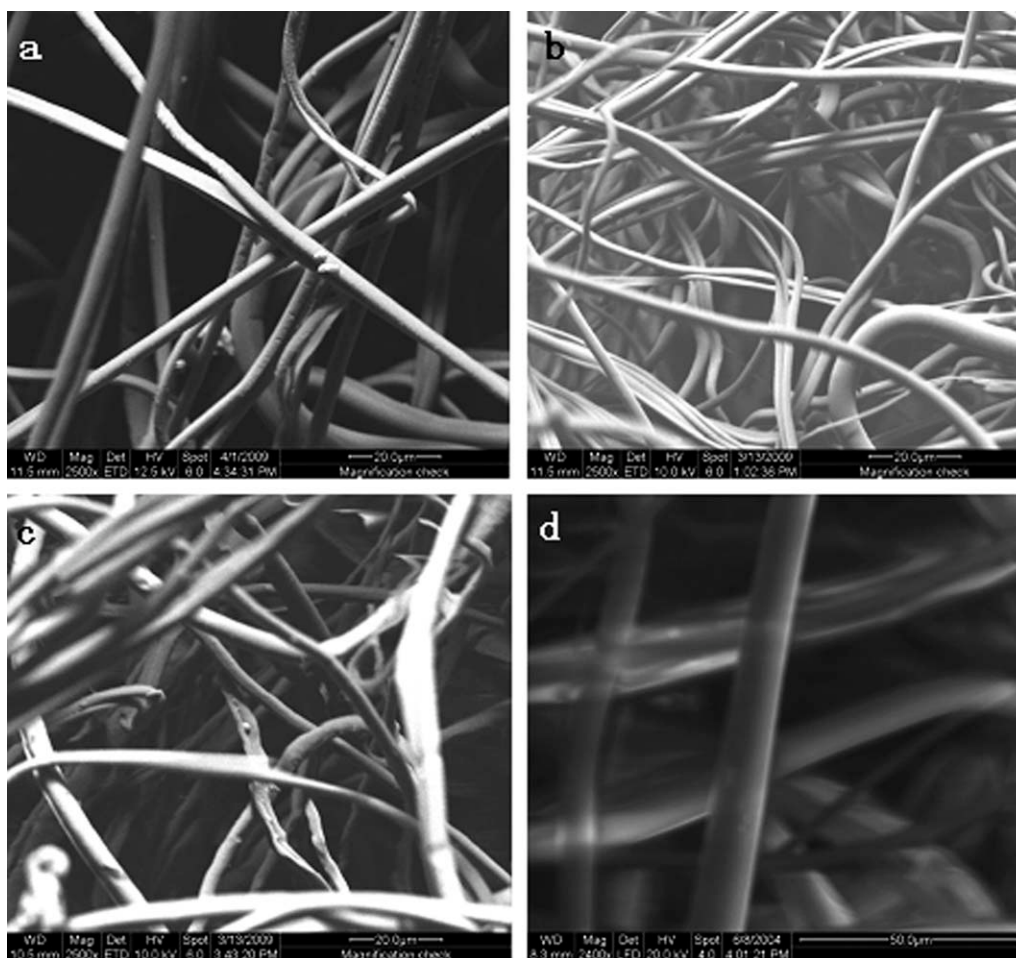


Figure 2 SEM images of different ratio PP/PET bi-MBs: (a) PP/PET 30/70, (b) PP/PET 50/50, (c) PP/PET 70/30, and (d) PP/PET 100/0.

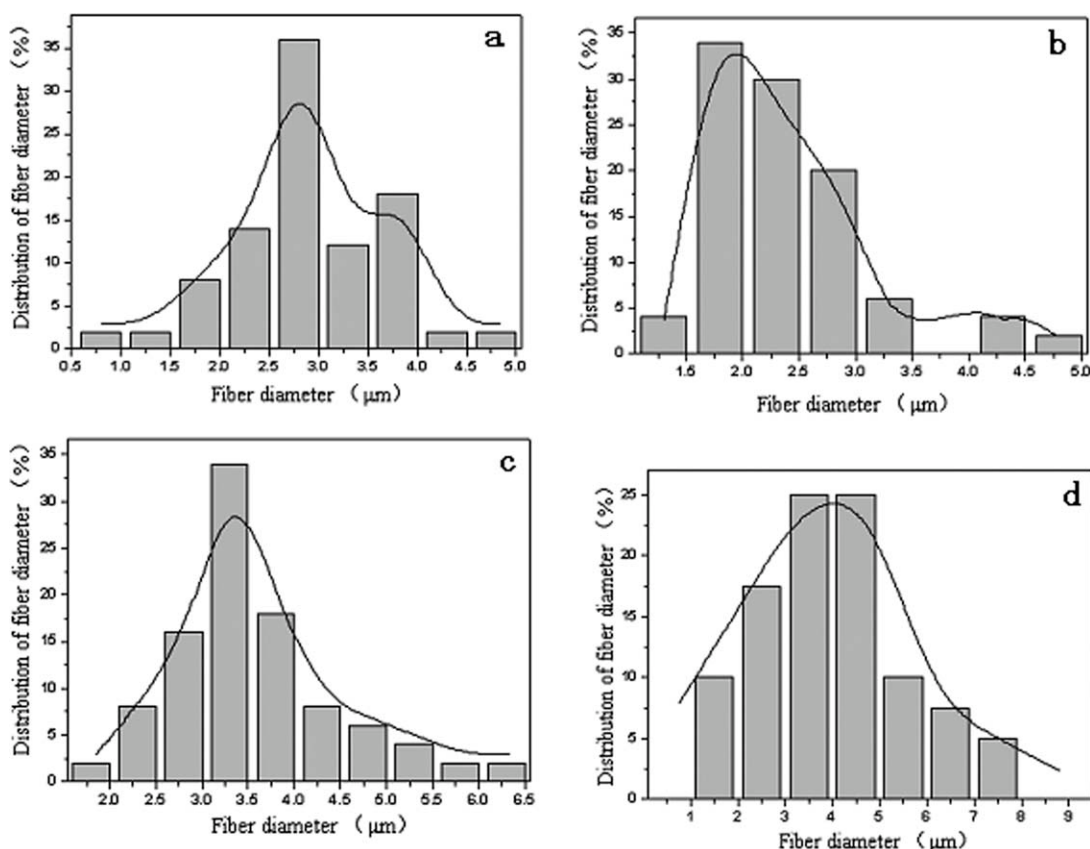


Figure 3 Fiber diameter distribution of different ratio PP/PET bi-MBs.

PP and 50% PET. So the fiber diameter was finest when the ratio of the two components was 50/50.

Mean pore size and porosity

It is very important to study the mean pore size and pore structure of nonwoven materials, especially materials used for filtration media. The pore size and structure directly affects the pressure drop, flow, and particle penetration performance.¹²

In this study, the mean pore size was tested through the PSM 165 pore size meter. According to eq. (1), the porosity was calculated with the method of weighted averages relative to the ratio of PP to PET. The results show in Table II.

It can be seen from Table II that the bi-MBs had a smaller mean pore size and higher porosity. Among these samples, the PP/PET ratio of 50/50 had the

smallest mean pore size and highest porosity, as shown in Figures 2 and 3, respectively. When the ratio of PP to PET was 50/50, the same ratio caused formation of an evenly split fiber during the cooling process, and the fiber diameter was finest. Meanwhile, the different thermal performances caused the formation of an obviously crimped fiber structure, which enabled the formation of fluffy structure during the web-forming stage, so the porosity increased, and the mean pore size decreased.

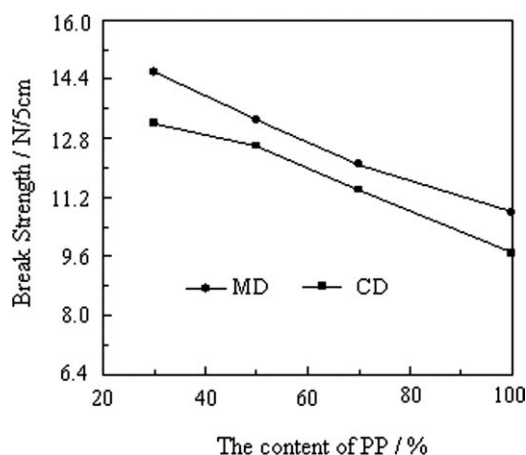


Figure 4 Break strength of different ratio PP/PET bi-MBs. MD = machine direction; CD = cross direction.

TABLE II
Mean Pore Size and Porosity Results of the PP/PET bi-MBs at Different Ratios

	30/70 PP/PET	50/50 PP/PET	70/30 PP/PET	100/0 PP/PET
Porosity (%)	90	94	92	85
Mean pore size (μm)	14.6	12.3	15.6	20.1

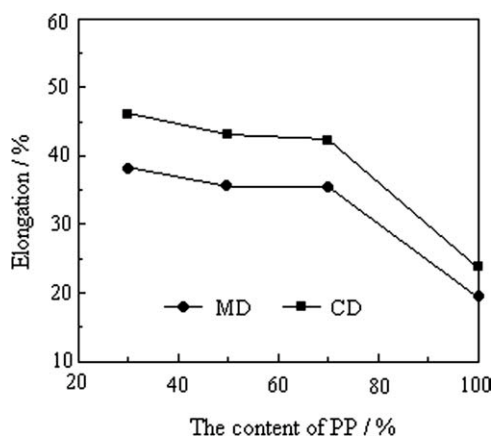
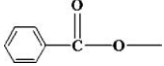


Figure 5 Elongation of different ratio PP/PET bi-MBs.

Mechanical performance

Figures 4 and 5 show the mechanical performance of different ratio PP/PET bi-MBs.

It can be seen from Figure 4 that the break strength of the bi-MBs was higher than that of the pure PP MBs. Meanwhile, with the increase of the PET content, the break strength increased. Because there was a  group in the PET molecular chain, the rigidity of the molecular chain turned higher; thus, the strength of the web improved, and it increased with the increase of the content of PET. Additionally, the fiber diameter was finer in the bi-MBs than in the mono MBs. Also, the cross section increased between fibers. The bond area increased after thermal bonding, so the slipped resistance turned higher, and the bi-MBs exhibited higher strength.

It can also be seen from Figure 5 that the elongation of the bi-MBs was higher than that of the pure

PP MBs. This phenomenon was derived from the crimped shape of the fiber, which enabled the higher flexibility of the bi-MBs, so they exhibited higher elongations when they broke.

Filtration performance

Table III shows the filtration performance of a single sheet of PP/PET bi-MBs. It can be seen from Table III that the filtration efficiency of the bi-MBs was higher than that of mono PP MBs, whereas the pressure drop was smaller. When the ratio of PP/PET was 50/50, the filtration efficiency reached the highest value; this was responsible to the former test data. Because the fiber was finer, the porosity was higher, and the pore size was smaller in the bi-MBs than in the mono PP MBs, the dispersion action was strong when the filtration carrier flowed through the fiber winding path. The particles that needed to be removed from the carrier had more chance to adhere to or impact the fiber. Meanwhile, the crimped fiber formed a three-dimensional netted random and fluffy structure, and the air carrier could pass successfully through the filter media. So, compared to the pure PP MBs, the bi-MBs had a higher filtration efficiency and lower pressure drop.

Because the bi-MBs were very thin, the filtration efficiency was improved, but it still could not reach the standard of high-efficiency filtration. A self-made cathode electric corona-discharge device was used to discharge the bi-MBs to produce corona-discharged bi-MBs. Through parameter control, the filtration efficiencies of the corona-discharged bi-MBs were calculated and are shown in Table IV.

It can be seen in Table IV that the filtration efficiency improved rapidly after corona discharge.

TABLE III
Filtration Efficiencies of the Single-Layer PP/PET bi-MBs

	Resistance (Pa)	Filtration efficiency (%)					
		$\geq 0.3 \mu\text{m}$	$\geq 0.5 \mu\text{m}$	$\geq 1 \mu\text{m}$	$\geq 3 \mu\text{m}$	$\geq 5 \mu\text{m}$	$\geq 10.0 \mu\text{m}$
30/70 PP/PET	9.82	40.58	52.25	59.21	79.65	94.54	96.25
50/50 PP/PET	13.12	50.34	64.43	71.36	83.47	98.63	99.42
70/30PP/PET	12.74	38.77	50.67	57.53	74.16	96.22	99.23
100/0 PP/PET	18.54	32.82	40.43	48.26	67.49	89.45	95.04

TABLE IV
Filtration Efficiencies of the Single-Layer PP/PET Corona-Discharged bi-MBs

	Resistance (Pa)	Filtration efficiency (%)					
		$\geq 0.3 \mu\text{m}$	$\geq 0.5 \mu\text{m}$	$\geq 1 \mu\text{m}$	$\geq 3 \mu\text{m}$	$\geq 5 \mu\text{m}$	$\geq 10.0 \mu\text{m}$
30/70 PP/PET	9.82	63.35	73.28	79.29	84.34	94.33	100.00
50/50 PP/PET	13.12	67.47	75.12	88.16	89.15	97.99	100.00
70/30PP/PET	12.74	61.59	66.82	75.53	83.29	93.22	100.00
100/0 PP/PET	18.54	59.15	64.28	72.17	80.16	90.45	99.56

TABLE V
Filtration Efficiencies of the Three-Layer PP/PET Corona-Discharged bi-MBs

	Resistance (Pa)	Filtration efficiency (%)					
		≥0.3 μm	≥0.5 μm	≥1 μm	≥3 μm	≥5 μm	≥10.0 μm
30/70 PP/PET	29.46	92.36	95.22	97.21	98.65	99.54	100.00
50/50 PP/PET	39.32	97.34	98.86	99.36	98.47	100.00	100.00
70/30 PP/PET	38.22	93.59	94.67	97.53	98.16	99.22	100.00
100/0 PP/PET	55.64	84.14	91.43	96.26	98.49	99.45	100.00

Because there was more charge in the bi-MBs after they were discharged, the static function was improved, and the charged dust could adhere to the bi-MBs; also, the polarized neutral particles were captured, and the filtration efficiency of the bi-MBs was improved. Among these samples, the sample of 50/50 PP/PET exhibited the highest filtration efficiency. Because this sample possessed the finest fiber diameter and smallest pore size, the surface electric charge density was the highest after corona discharge.

According to the filtration model established by Qinfei Ke of Donghua University, if we divided the filtration media into several layers, the number of particles in every layer would be decreased along the filtration direction.¹³ This theory shows that the filtration efficiency would not be affected by the thickness when it reached a certain degree, so we put three layers of bi-MBs together for the filtration performance test in this research. The test results are shown in Table V.

It can be seen from Table V that the filtration efficiency improved remarkably when the three layers were put together. The filtration efficiency for 0.3-μm dust particles reached 97.34% in the 50/50 PP/PET sample. The layer increase made the hole winded and mutative, and the block ability of the particles improved, so the filtration efficiency improved obviously.

Air permeability

Air permeability is another performance index of filter media. For fibrous filter media, the air permeability is determined by the size and number of pores in the web. The air permeability is excellent if the pore size is bigger and the porosity is higher.¹⁴ Also, it is related to the diameter and structure of the fiber. The air permeability test results are shown in Table VI.

TABLE VI
Air Permeabilities of the PP/PET Corona-Discharged bi-MBs

	30/70 PP/PET	50/50 PP/PET	70/30 PP/PET	100/0 PP/PET
Air permeability (L·m ⁻² ·s ⁻¹)	969.8	1206.0	1068.2	940.1

It can be seen from Table VI that the air permeability of the PP/PET bi-MBs was better than that of the mono PP MBs. As discussed earlier, the air permeability was determined by the size and number of pores in the web. Although the mean pore size of the PP/PET bi-MBs was smaller than that of the mono PP MBs, the porosity was higher than that of the mono PP MBs; they exhibited excellent air permeability when the filtration carrier flowed through.

CONCLUSIONS

Compared with the single-component MBs, in the bi-MBs, the fiber diameter was finer, the surface area was bigger, the pore size was smaller, and the porosity was higher. Also, the fiber was crimped to form a three-dimensional structure, which was particularly beneficial for filtration.

Also, when the PP/PET ratio was 50/50, the fiber had the finest diameter of 2.34 μm. The web had the biggest porosity of 94%, and the lowest mean pore size was 12.3 μm. This led to a low filtration resistance and high filtration efficiency. After the corona-discharge process, the filtration efficiency (for the particulate < 0.3 μm) could reach 97.34%, and the air permeability could reach 1206.0 L·m⁻²·s⁻¹, and this material could be used as high-performance filter media.

References

- Zhang, D.; Sun, Q.; Song, H. *J Appl Polym Sci* 2004, 94, 1218.
- Liu, Y. J.; Hou, M. Y.; Xiao, X. X. *China Text Leader* 2006, 8, 79.
- Li, Y. M.; Cheng, B. W.; Liu, Y. *Tech Text* 2007, 7, 5.
- Liu, W. S. *Chem Fiber Text Technol* 2007, 4, 33.
- Qian, W. F. *Shanghai Text Sci Technol* 2005, 5, 62.
- Wilkie, A. E. *Int Fiber J* 2006, 21, 38.
- Zhang, D.; Sun, Q.; Beard, J.; et al. *J Appl Polym Sci* 2002, 83, 1280.
- Sun, Q.; Zhang, D. *Tech Text* 2005, 11, 9.
- Sun, Q.; Zhang, D.; Liu, Y. B.; et al. *J Appl Polym Sci* 2004, 93, 2090.
- Zhao, R. G.; Wadsworth, L. C.; Sun, Q.; et al. *Polym Int* 2003, 52, 133.
- Zhou, R.; Zhao, Y. Z. *Beijing Text J* 2002, 3, 17.
- Pan, Y.; Wang, S. Y. *J China Text Univ* 2000, 26, 73.
- Ke, Q. F. *Tech Text* 2000, 5, 1.
- Zhang, J. Z.; Gao, Y. N. *J Filtr Sep* 2006, 2, 39.